

Visual Servo Velocity and Pose Control of a Wheeled Inverted Pendulum through Partial-Feedback Linearization

Nicholas R. Gans

Dept. of Mechanical and Aerospace Engineering
University of Florida
Gainesville, FL USA
Email: ngans@ufl.edu

Seth A. Hutchinson

Dept. of Electrical and Computer Engineering
University of Illinois Urbana Champaign
Urbana, IL USA
Email: seth@uiuc.edu

Abstract—Vision-based control of wheeled vehicles is a difficult problem due to nonholonomic constraints on velocities. This is further complicated in the control of vehicles with drift terms and dynamics containing fewer actuators than velocity terms. We explore one such system, the wheeled inverted pendulum, embodied by the Segway. We present two methods of eliminating the effects of nonactuated attitude motions and a novel controller based on partial feedback linearization. This novel controller outperforms a controller based on typical linearization about an equilibrium point.

I. INTRODUCTION

Many mobile robots fall into the category of nonholonomic vehicles, which are typically underactuated and have constraints on derivatives of the configuration variables. Typical feedback control methods offer poor results or may not work at all. The field of nonholonomic motion planning has grown to address these issues [1].

The use of computer vision to control nonholonomic systems has been explored. Pissard-Gibollet and Rives [2] detailed the problems of using vision-based control with nonholonomic vehicles and overcome these problems by adding additional degrees of freedom to the camera. Ma et al. [3] established vision-based feedback control of a unicycle and car-like robots using advanced techniques in nonholonomic path planning. Fang et al. [4] controlled a mobile robot using Position Based Visual Servoing techniques based on planar homography. The authors developed a stable, vision-based controller for unicycle-like robots utilizing a switched system approach [5], [6].

Problems are compounded when a system with nonholonomic constraints must be described by a set of dynamic equations. In this case, drift terms generally exist and motions along the nonactuated degrees of freedom may accompany desired, actuated motions. For a system using vision, drift and motions along nonactuated degrees of freedom are particularly troublesome, as small unwanted camera motions can dramatically alter the image.

In this paper we focus on the situation of a wheeled inverted pendulum (WIP), similar to the Segway vehicle, using angle

sensors to control the pitch and camera data to control pose and velocity. The motion of the WIP is described by a set of second order differential equations and is subject to nonholonomic constraints. To implement a vision based controller we must deal with the problem of nonactuated motions affecting the image.

We explore and implement three methods to counter this problem. These methods can be used in conjunction with each other to improve performance. First is to simply design a better controller to reduce drift and undesired motions. To this end we design a controller through partial feedback linearization that provides strong regulation of the WIP balance.

A second method is to find a set of features that are not affected by motions along nonactuated degrees of freedom. Hamel and Mahony [7] take this approach to control the pose of a helicopter-like robot. We present a set of features that are not strongly affected by pitch rotations, such as when the WIP tips and rocks during normal operation. The third method is to subtract the effects of unwanted motions from the features. Given an angle sensor, such as a rate-gyro, it is possible to sense the pitch angle of the camera attached to the WIP and correct the features as if there was no pitch.

In Section II we introduce the WIP and present two controllers, one involving linearization about an equilibrium, and one using a novel partial-feedback linearization. In Section III we discuss methods of handling the effects of nonactuated pitch angle on the image. In Section IV, we present simulations of the above method for a vision-based control task along a complicated trajectory.

II. WHEELED INVERTED PENDULUM

A. Background

Vehicles characterized as wheeled inverted pendulums (WIP's) have received recent attention in the robotics community [8], [9]. A WIP is a body above two wheels with no balancing support. We define a world frame with the z -axis oriented up. We define a body frame, denoted with the subscript b , with origin at the midpoint between the wheels and oriented such that the y_b -axis is colinear with the wheel

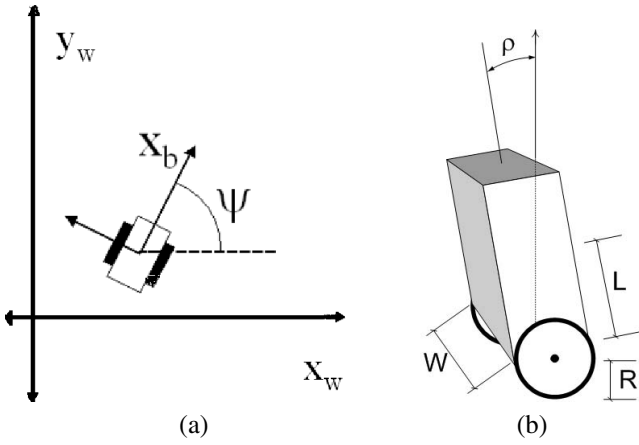


Fig. 1. Diagrams of the Wheeled Inverted Pendulum Robot

axle and the z_b -axis is always parallel to the world z -axis (the body frame does not tip with the WIP). Under the assumption that the tires do not slip, the x_b -axis of this frame points in the direction of linear velocity v . This is illustrated in Figure 1.

The WIP has state variables $[x, y, \psi, \rho]^T$ where x and y are the position of the robot in the plane, ψ is the bearing angle measured from the world x -axis to the body x -axis, and ρ is the attitude, or pitch, angle measured from the z -axis. However, the distribution of available velocities is of rank two. The WIP has three degrees of freedom but only two actuators.

The motion of the WIP is described by a set of second order differential equations that include the constant influence of gravity. Due to nonholonomic constraints, there does not exist a smooth feedback control for asymptotic stabilization to a point in the state space. Physical characteristics of interest in the sequel include: wheel radius, R ; wheel base length, W ; length to mass center, L ; body mass M_b and moment of inertia in the pitch direction, I_ρ . The WIP is diagrammed in Figure 1(a) and (b).

To implement the switched system controller, we first need a controller for the WIP which can drive and steer while regulating the attitude around zero. Our design is based upon the work of Baloh and Parent[9]. We will not reproduce their work here, but refer to their paper for the full derivation of the equations of motion. They take three generalized coordinates

$$\mathbf{q}^T = [\theta_{lw}, \theta_{rw}, \rho]^T \quad (1)$$

where θ_{lw} and θ_{rw} are the angles of the left and right wheel, respectively.

Following standard practice, the dynamic equations can be written as

$$\mathbf{H}(\mathbf{q})\ddot{\mathbf{q}} + \mathbf{C}(\dot{\mathbf{q}}, \mathbf{q}) + \mathbf{G}(\mathbf{q}) = \mathbf{Q}\mathbf{u}. \quad (2)$$

$\mathbf{H}(\mathbf{q})$ is the inertia matrix, $\mathbf{C}(\dot{\mathbf{q}}, \mathbf{q})$ is a vector containing damping terms, $\mathbf{G}^T = [0, 0, M_b g L \sin(\rho)]^T$ collect external

forces, g is the acceleration of gravity and

$$\mathbf{Q}\mathbf{u} = \beta \begin{bmatrix} 1 & 0 \\ 0 & 1 \\ 1 & 1 \end{bmatrix} \begin{bmatrix} \tau_{lw} \\ \tau_{rw} \end{bmatrix} \quad (3)$$

where β incorporates various characteristics of the motors, and τ_{lw} and τ_{rw} are the torques on the right and left wheel.

B. Control Through Linearization About a Point

The simplest approach is to multiply both sides of (2) by \mathbf{H}^{-1} and linearize about the point $\mathbf{q} = [0, 0, 0]^T$. This was investigated by Chen, et al. in a technical report [10].

The linearized system can be expressed in a state-space model by

$$\begin{bmatrix} \dot{\theta}_{rw} \\ \ddot{\theta}_{rw} \\ \dot{\theta}_{lw} \\ \ddot{\theta}_{lw} \\ \dot{\rho} \\ \ddot{\rho} \end{bmatrix} = \begin{bmatrix} 0 & 1 & 0 & 0 & 0 & 0 \\ 0 & 0 & 0 & 0 & a_1 & 0 \\ 0 & 0 & 0 & 1 & 0 & 0 \\ 0 & 0 & 0 & 0 & a_1 & 0 \\ 0 & 0 & 0 & 0 & 0 & 1 \\ 0 & 0 & 0 & 0 & a_2 & 0 \end{bmatrix} \begin{bmatrix} \theta_{rw} \\ \dot{\theta}_{rw} \\ \theta_{lw} \\ \dot{\theta}_{lw} \\ \rho \\ \dot{\rho} \end{bmatrix} + \begin{bmatrix} 0 & 0 \\ b_1 & b_2 \\ 0 & 0 \\ b_2 & b_1 \\ 0 & 0 \\ b_3 & b_3 \end{bmatrix} \begin{bmatrix} \tau_{rw} \\ \tau_{lw} \end{bmatrix} \quad (4)$$

Where a_1 , a_2 , b_1 , b_2 and b_3 depend on physical characteristics and will vary between different WIP robots.

Assuming full state feedback, feedback gains can be solved by using LQR optimal design techniques. The system will be stabilized about the the optimal point $\mathbf{q} = [0, 0, 0]^T$. To drive and steer, desired velocities in the robot frame v and ω can be mapped to desired values of \mathbf{q} and $\dot{\mathbf{q}}$

$$v = R/2(\dot{\theta}_{lw} + \dot{\theta}_{rw}) \quad (5)$$

$$\omega = R/W(\dot{\theta}_{lw} - \dot{\theta}_{rw}) \quad (6)$$

$$\theta_{lw} = -\theta_{rw} \quad (7)$$

$$\dot{\theta}_{lw} = v/R + \omega W/2R \quad (8)$$

$$\theta_{rw} = -\theta_{lw} \quad (9)$$

$$\dot{\theta}_{rw} = v/R - \omega W/2R \quad (10)$$

C. Control Through Feedback Linearization

Improved performance was sought using partial feedback linearization [11], [12]. Pathak, et al. developed a WIP control using partial feedback linearization, however they followed a different development tactic and used a world reference frame. Our system expresses equations in a reference frame attached to the robot. Subsequently our equations are simpler and well suited to control schemes that involve on board sensors such as mounted cameras.

We note that the generalized coordinates, \mathbf{q} , are not particularly intuitive for velocity control. Equations (1),(5) and (6),

$\dot{x}_b = v$, and $\dot{\psi} = \omega$ can be combined to give

$$\begin{bmatrix} \dot{x}_b \\ \dot{\psi} \\ \dot{\rho} \end{bmatrix} = \begin{bmatrix} R/2 & R/2 & 0 \\ R/W & -R/W & 0 \\ 0 & 0 & 1 \end{bmatrix} \begin{bmatrix} \dot{\theta}_{lw} \\ \dot{\theta}_{rw} \\ \dot{\rho} \end{bmatrix} \quad (11)$$

$$\dot{\mathbf{x}} = \mathbf{J}_x \dot{\mathbf{q}}. \quad (12)$$

Since \mathbf{J}_x is a constant matrix, we also have

$$\ddot{\mathbf{x}} = \mathbf{J}_x \ddot{\mathbf{q}} \quad (13)$$

We can use this Jacobian to transform (2) to

$$\mathbf{H}_x(\mathbf{x})\ddot{\mathbf{x}} + \mathbf{C}_x(\dot{\mathbf{x}}, \mathbf{x}) + \mathbf{G}_x(\mathbf{x}) = \mathbf{u}_x, \quad (14)$$

where $\mathbf{H}_x = \mathbf{J}_x \mathbf{H} \mathbf{J}_x^{-1}$, $\mathbf{C}_x = \mathbf{J}_x \mathbf{C}$, $\mathbf{G}_x = \mathbf{J}_x \mathbf{G} = \mathbf{G}$, and

$$\mathbf{u}_x = \beta \begin{bmatrix} R/2 & R/2 \\ R/W & -R/W \\ 1 & 1 \end{bmatrix} \begin{bmatrix} \tau_{lw} \\ \tau_{rw} \end{bmatrix}.$$

We note that the angle ρ is not independently actuated, but is scaled from the input for x_b . From the classic inverted pendulum problem, it is seen that

$$(I_\rho + M_b L^2) \ddot{\rho} = M_b L \cos(\rho) \ddot{x}_b + M_b g L \sin(\rho).$$

The term $(I_\rho + M_b L^2)$ is contained in the third diagonal term of \mathbf{H}_x and $M_b g L \sin(\rho)$ is the only nonzero term of \mathbf{G}_x . We can thus augment the \mathbf{H}_x and \mathbf{u}_x terms as

$$\mathbf{H}'_x = \mathbf{H}_x(\mathbf{x}) + \begin{bmatrix} 0 & 0 & 0 \\ 0 & 0 & 0 \\ M_b L \cos(\rho) & 0 & 0 \end{bmatrix}$$

$$\mathbf{u}'_x = \begin{bmatrix} R/2 & R/2 \\ R/w & -R/w \\ 0 & 0 \end{bmatrix} \begin{bmatrix} \tau_{lw} \\ \tau_{rw} \end{bmatrix}$$

The system

$$\mathbf{H}'_x \ddot{\mathbf{x}} + \mathbf{C}_x(\dot{\mathbf{x}}, \mathbf{x}) + \mathbf{G}_x(\mathbf{x}) = \mathbf{u}'_x \quad (15)$$

is finally in a form to which we can apply partial feedback linearization. We separate the actuated variables x_b and ψ from the nonactuated variable ρ by separating the top two rows of the matrices from the bottom row. We rewrite Equation (15) as

$$\mathbf{H}_{11} \begin{bmatrix} \ddot{x}_b \\ \ddot{\psi} \end{bmatrix} + \mathbf{H}_{12} \ddot{\rho} + \mathbf{C}_1 = \mathbf{u}'_x \quad (16)$$

$$\mathbf{H}_{21} \begin{bmatrix} \ddot{x}_b \\ \ddot{\psi} \end{bmatrix} + H_{22} \ddot{\rho} + C_2 + G = 0. \quad (17)$$

Where terms that evaluate to scalars are no longer in bold.

Solving for $\ddot{\rho}$ as

$$\ddot{\rho} = -H_{22}^{-1} \left[\mathbf{H}_{21} \begin{bmatrix} \ddot{x}_b \\ \ddot{\psi} \end{bmatrix} + C_2 + G \right]$$

and substituting into (16) gives

$$\bar{\mathbf{H}}(\mathbf{x}) \begin{bmatrix} \ddot{x}_b \\ \ddot{\psi} \end{bmatrix} + \bar{\mathbf{F}}(\mathbf{x}, \dot{\mathbf{x}}) = \mathbf{u}'_x \quad (18)$$

where

$$\bar{\mathbf{H}} = \mathbf{H}_{11} - H_{22}^{-1} \mathbf{H}_{12} \mathbf{H}_{21}$$

$$\bar{\mathbf{F}} = \mathbf{C}_1 - H_{22}^{-1} \mathbf{H}_{12} (C_2 + G).$$

Using the feedback control law

$$\mathbf{u}'_x = \bar{\mathbf{H}} \begin{bmatrix} a \\ \alpha \end{bmatrix} + \bar{\mathbf{F}}, \quad (19)$$

where a and α are desired linear and angular velocity, respectively, and using the fact that the second element of \mathbf{H}_{21} is 0, we rewrite Equations (16) and (17) as

$$\begin{bmatrix} \ddot{x}_b \\ \ddot{\psi} \end{bmatrix} = \begin{bmatrix} a \\ \alpha \end{bmatrix} \quad (20)$$

$$\ddot{\rho} = -H_{22}^{-1} (H_{21}(1) \ddot{x}_b + C_2 + G) \quad (21)$$

We can regulate ρ through x_b . A simple, but highly effective method is to use proportional state feedback with $\dot{\rho}$ and ρ . Assuming, for the moment, that $[\ddot{x}_b, \ddot{\psi}]^T = [\dot{x}_b, \dot{\psi}]^T = [0, 0]^T$, we use

$$\ddot{\rho} = -K_1 \dot{\rho} - K_2 \rho \Rightarrow$$

$$\ddot{x}_b = -H_{21}(1)^{-1} [C_2 + G - H_{22} (K_1 \dot{\rho} - K_2 \rho)] \quad (22)$$

where K_1 and K_2 are gains.

Combining (20), (21), (22) and $[a, \alpha]^T = [0, 0]^T$ gives the final, zero-input state equations

$$\begin{bmatrix} \ddot{x}_b \\ \ddot{\psi} \\ \ddot{\rho} \end{bmatrix} = \begin{bmatrix} -H_{21}(1)^{-1} [C_2 + G - H_{22} (K_1 \dot{\rho} - K_2 \rho)] \\ 0 \\ -K_1 \dot{\rho} - K_2 \rho \end{bmatrix}. \quad (23)$$

When $[a, \alpha]^T \neq [0, 0]^T$ the state is described by the equations

$$\begin{bmatrix} \ddot{x}_b \\ \ddot{\psi} \\ \ddot{\rho} \end{bmatrix} = \begin{bmatrix} a - H_{21}(1)^{-1} [C_2 + G - H_{22} (K_1 \dot{\rho} - K_2 \rho)] \\ \alpha \\ -K_1 \dot{\rho} - K_2 \rho \end{bmatrix} \quad (24)$$

When ρ is small the state acceleration is very close to the input acceleration, and ρ regulated to 0 as well.

To illustrate the superior attitude control of the partial-feedback linearized system, see Figure 2. This graph shows a simulation of attitude of the robot under both controllers while balancing in place. The partial-feedback linearize system is clearly much better regulated about $\rho = 0$. The attitude was simulated again under a constant requested input of $v = .5$ m/sec and $\omega = 1$ rad/sec to show regulation during motion, and is shown in Figure 3. The feedback linearized system is much smoother, but there is an additional interesting feature. The feedback linearized system has a positive ρ , meaning it keeps WIP tilted forward, which accommodates a steady state ρ at a steady v . The typically linearized system has a negative ρ , meaning the WIP leans backwards and is "dragged" behind the wheels. There is no steady state ρ associated with this configuration, so the robot must repeatedly alter its speed to keep the WIP from falling. However, the average magnitude of the attitude is less for the linearized system, which could be

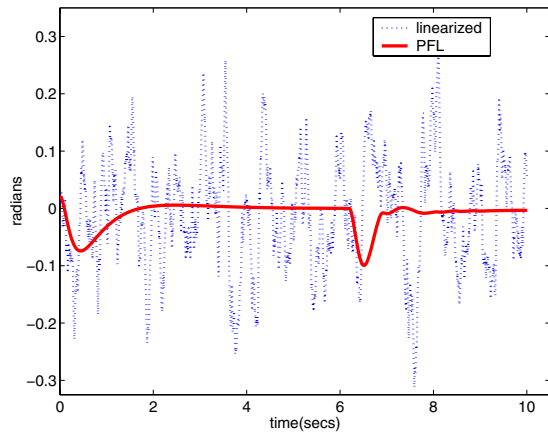


Fig. 2. Values of ρ for both WIP control systems with zero input

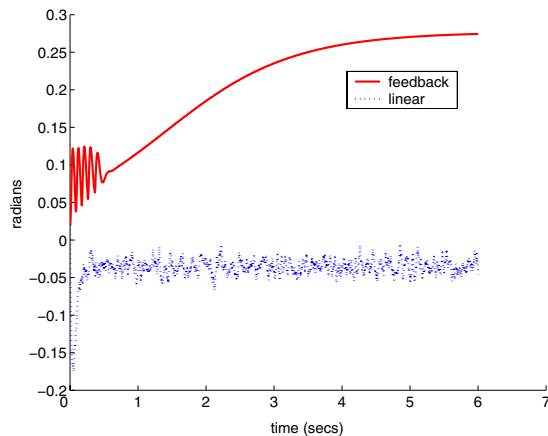


Fig. 3. Values of ρ for both WIP control systems with constant velocity input

a consideration. The feedback linearized system also allows for closed loop control of the velocity, while the traditional linearized system is effectively an open loop velocity control. Further comparisons will be given in Section IV, after a vision based control task has been introduced.

III. VISION BASED CONTROL OF A TWO-WHEELED INVERTED PENDULUM ROBOT

Vision-based control of mobile robots is a continually growing field. Cameras can be used to provide data that is used in path planning. Alternately, camera data can be used in the feedback loop of a controller, a process known as visual servoing (VS) [13], [14], [15], [16]. Visual servoing generally assumes a kinematic model, and is ill suited for control of dynamic systems that do not have control over all degrees of freedom.

Consider a camera mounted on a WIP. The camera frame is fixed such that the horizontal axis of the image plane is always parallel to y_b of the WIP, and when $\rho = 0$, the optical axis is aligned with x_b and the image vertical axis is aligned with z_b . A 3D point \mathbf{P} will project to a point \mathbf{p} in the image with horizontal and vertical coordinates $\mathbf{p} = [h, n]^T$, as described

by the pinhole camera model.

The WIP has three degrees of freedom, with velocity vector

$$\xi = [v, \omega, \dot{\rho}]^T. \quad (25)$$

Motion of the WIP will cause motion of \mathbf{p} in the image according to

$$\begin{bmatrix} \dot{h} \\ \dot{n} \end{bmatrix} = \begin{bmatrix} -\frac{h}{z} & \frac{\lambda^2 + h^2}{\lambda} & -\frac{hn}{\lambda} \\ -\frac{n}{z} & \frac{hn}{\lambda} & -\frac{\lambda^2 - n^2}{\lambda} \end{bmatrix} \begin{bmatrix} v \\ \omega \\ \dot{\rho} \end{bmatrix} \quad (26)$$

$$\dot{\mathbf{p}} = \mathbf{L}_i \xi \quad (27)$$

where z is the depth of the point in the image frame, λ is the focal length of the camera, and \mathbf{L}_i is the *interaction matrix* or *image Jacobian*[14], [13], [15], [16].

The first concern when using visual servoing to control an underactuated, dynamic system is motion along the uncontrolled degrees of freedom. In the case of the WIP, changes in the system attitude ρ will occur due to the constant effects of gravity and will accompany any linear accelerations. Small changes in attitude can cause large motions of features in the image space. This is particularly troublesome to image-based visual servo controllers. There are several ways to address this concern, which can be used in conjunction.

The first method is to insure that nonactuated motions are as small and infrequent as possible. In Section II-C we introduced a controller, based on partial feedback linearization, that regulates $\dot{\rho}$ very well. At zero input, $\dot{\rho}$ is very near zero, and during accelerations the motion of ρ is smooth.

A second approach is to subtract the image error that corresponds to motion along the uncontrolled degrees of freedom. This can be done so long as such motions can be independently sensed. In the case of the WIP, ρ can be sensed through the use of a rate-gyro and/or tilt sensor. A “corrected” feature point is given by

$$\mathbf{p}' = \mathbf{p} - \begin{bmatrix} -\frac{hn}{\lambda} \\ -\frac{\lambda^2 - n^2}{\lambda} \end{bmatrix} \rho \quad (28)$$

Figure 4 demonstrates removing the effects of pitch from an image. Figure 4(a) shows a side view demonstrating a collection of feature points in front of the WIP robot, which is pitching forward. The camera is mounted 3/4 of the way up the robot body. Figure 4(b) shows the camera’s view. Circles are the feature points in the image if there was no pitch. Diamonds show the current camera view of the points, and squares are the current view with the effects of pitch removed.

Another approach is to choose features, possibly other than points, that are not affected by the uncontrolled motions. This method lends itself particularly to image-based methods which can use a wide variety of features. Hamel and Mahony take this approach in developing a visual servo control for a helicopter-like vehicle [7]. One drawback to this approach is that often such a set of features cannot offer control over all degrees of freedom, and non-image-based information must be used as

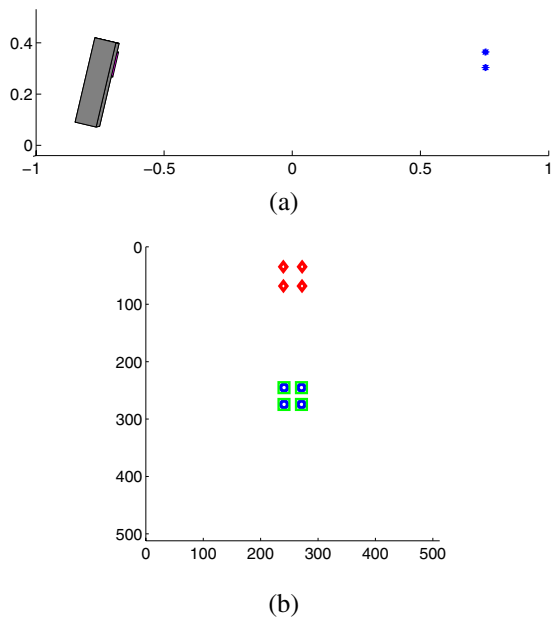


Fig. 4. Example of Subtracting the Effects of Pitch from an Image

well. In the case of Hamel's and Mahony's helicopter, constant knowledge of the direction of gravity was necessary.

For the WIP, one possible alternate set of features is to use only the horizontal coordinates, h , of a set of feature points. This is feasible since we are controlling only two degrees of freedom, so the horizontal position in the image of two feature points is sufficient for IBVS methods, so long as the horizontal coordinates are not equal. The horizontal coordinate is invariant to translation along the vertical camera axis, and highly invariant to rotation about the horizontal camera axis.

In Figure 5 we show the coordinates of image points over time for a camera mounted on a WIP balanced through standard linearization about $\rho = 0$, which shows more pitch than the feedback linearization. The top graph shows the h and n coordinates for typical feature points. The h component remains small, as it is not affected strongly by pitch, while the n component moves by over 150 pixels. The second graph shows the same points after being corrected by removal of the motion due to the pitch. The n components now never move more than 5 pixels, the h components show some motion due to drift of the WIP, which was not noticeable in the first graph due to the scale. The third graph shows just the h coordinates. Naturally, it is very similar to the h component of the corrected points.

IV. RESULTS

We have performed simulations to test the above ideas. Our task is based on a vision-based control algorithm we have previously developed [5], [6]. This algorithm is similar in spirit and form to one independently developed by Kantor and Rizzi [17].

The robot performs a series of motions to move around an annulus while keeping a landmark in the field of view, similar to a parallel parking problem.

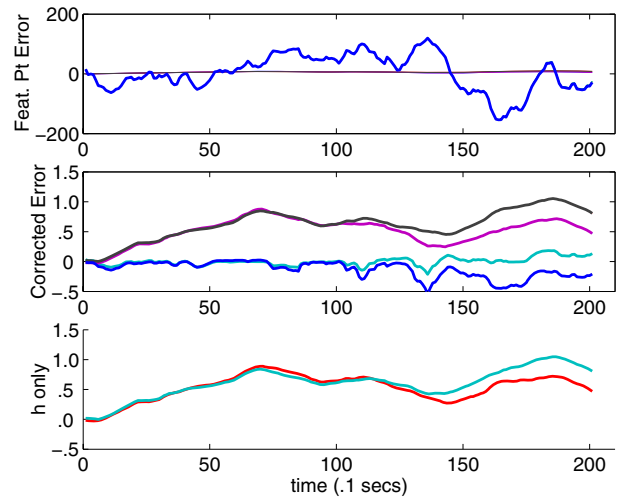


Fig. 5. Examples of Feature Errors for balancing WIP

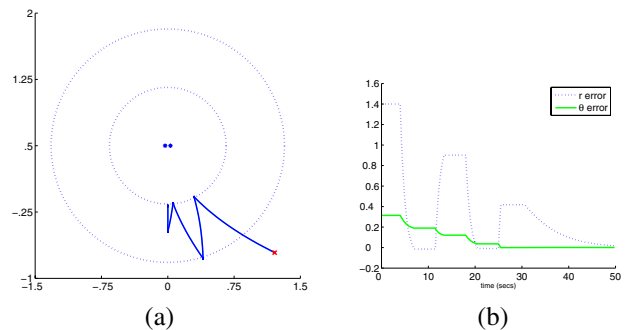


Fig. 6. Trajectory and Error Values for Simulation of Kinematic Unicycle

We refer the reader to our other publications for details on the control algorithm. Suffice to say, it involves a series of rotations and driving along curves. These velocities are based on image feature errors and a distance measurement to the landmark, similar in spirit to classical image-based visual servo methods. The algorithm was developed for a kinematic unicycle type robot. The kinematic unicycle is similar to a WIP, but there is no ρ motion and dynamics can be neglected. This also means there is no drift or nonactuated motion. When implemented on a WIP, we look to see how well the controller can match the performance of the kinematic system.

Graphs of the task for a kinematic model are shown in Figure 6. Figure 6(a) shows a top-down view of the trajectory of the robot around the annulus from a start position at the lower right to a goal position in front of a landmark consisting of dots in the center of the figure. Figure 6(b) shows the position error in terms of polar coordinates r and θ .

Results of the same task with the traditionally linearized WIP controller, with pitch removed from the feature points is shown in Figure 7. Figure 7(a) shows the trajectory of the WIP robot over time; Figure 7(b) shows the error in r and θ over time. The trajectory appears very similar to that for the kinematic model, but the pose error differs quite a bit. It also

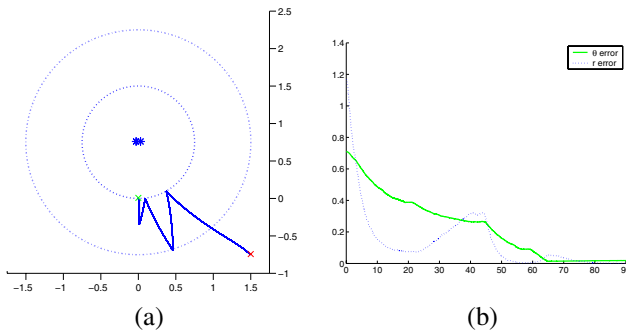


Fig. 7. Trajectory and Error Values for Simulation of Linearized WIP

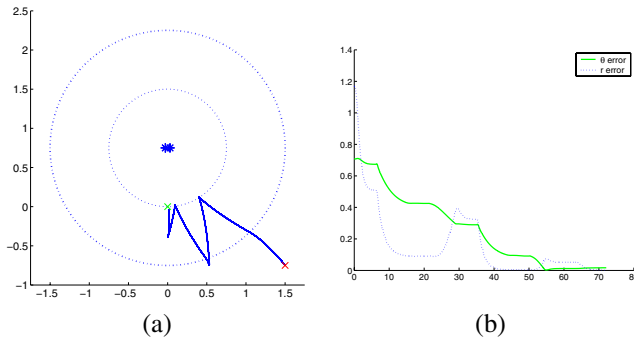


Fig. 8. Trajectory and Error Values for Simulation of Partial-Feedback Linearized WIP

takes almost twice as long as the kinematic model to complete.

Simulations have been conducted for the partial-feedback linearized model as well. Figure 8(a) shows the trajectory of the WIP robot over time, and Figure 8(b) shows the error in r and θ . Comparing these results to those of the kinematic unicycle, the trajectories of the systems are very similar. The error functions are much closer to the kinematic model than those of the traditional linearized model. It outperforms the traditional linearized system in control of the attitude and the time needed to complete the task.

V. CONCLUSION

Vision-based control of mobile robots is made more difficult in the presence of nonholonomic constraints, particularly when the system must be described by a dynamic model. In this case there will often be nonactuated motions that will affect the image. We have presented two methods of reducing the effects on nonactuated motions on the image. These methods can generally be applied to dynamic vehicle if certain pose sensors or assumptions on the vehicle motions can be met.

For the specific case of a wheeled inverted pendulum, we have also presented a novel controller using partial feedback linearization. This model provides dramatic improvement in control over a controller designed with traditional linearization about an equilibrium point. This improvement is particularly strong in regulating nonactuated motions, which improves vision-based control.

We have presented simulations to demonstrate the strengths of our proposals with a visual servoing control task that

involves several changes of direction. Further work should be done to compare the merits of each proposals individually. Implementation of these controllers on a WIP robot could follow as well.

VI. ACKNOWLEDGMENTS

This material is based in part upon work supported by the National Science Foundation under Award Nos. CCR-0085917 and IIS-0083275.

REFERENCES

- [1] J. Laumond and J. Risler, "Nonholonomic systems: controllability and complexity," 1996.
- [2] R. Pissard-Gibollet and P. Rives, "Applying visual servoing techniques to control a mobile hand-eye system," in *Proc. of the International Conference on Robotics and Automation*, vol. 1, pp. 166 – 171, 1995.
- [3] Y. Ma, J. Kosecka, and S. Sastry, "Vision guided navigation for a nonholonomic mobile robot," *IEEE Transactions on Robotics and Automation*, vol. 15, no. 3.
- [4] Y. Fang, D. Dawson, W. Dixon, and M. de Queiroz, "Homography-based visual servoing of wheeled mobile robots," in *2002, Proc. IEEE Conf. on Decision and Control*, pp. 2866 – 2871, 2002.
- [5] S. Bhattacharya, R. Murrieta-Cid, and S. Hutchinson, "Path planning for a differential drive robot: Minimal length paths-a geometric approach," in *Proc. Int. Conf. Intelligent Robots and Systems*, 2004.
- [6] N. R. Gans, *Hybrid Switched System Visual Servo Control*. PhD thesis, University of Illinois Urbana-Champaign, 2005.
- [7] T. Hamel and R. Mahony, "Visual servoing of an under-actuated dynamic rigid-body system: an image-based approach," *IEEE Transactions on Robotics and Automation*, pp. 187 – 198, 2002.
- [8] K. Pathak, J. Franch, and S. Agrawal, "Velocity and position control of a wheeled inverted pendulum by partial feedback linearization," 2005.
- [9] M. Baloh and M. Parent, "Modeling and model verification of an intelligent self-balancing two-wheeled vehicle for an autonomous urban transportation system," in *Proc. Conf. on Computational Intelligence, Robotics, and Autonomous Systems*, 2003.
- [10] D. Chen, E. Bettini, C. Graesser, A. Block, and C. Montesinos., "The segbot-technical report for introduction to mechatronics class project." <http://coecsl.ece.uiuc.edu/ge423/spring04/group9/objectives.htm>, May 2005.
- [11] M. W. Spong, "Partial feedback linearization of underactuated mechanical systems," in *Proc. Int. Conf. Intelligent Robots and Systems*, pp. 314–321, Sep 1994.
- [12] M. Reyhanoglu, A. van der Schaft, N. Mcclamroch, and I. Kolmanovskiy, "Dynamics and control of a class of underactuated mechanical systems," 1999.
- [13] L. E. Weiss, A. C. Sanderson, and C. P. Neuman, "Dynamic sensor-based control of robots with visual feedback," *IEEE Journal of Robotics and Automation*, vol. RA-3, pp. 404–417, Oct. 1987.
- [14] J. Feddema and O. Mitchell, "Vision-guided servoing with feature-based trajectory generation," *IEEE Transactions on Robotics and Automation*, vol. 5, pp. 691–700, Oct. 1989.
- [15] B. Espiau, F. Chaumette, and P. Rives, "A new approach to visual servoing in robotics," *IEEE Trans. on Robotics and Automation*, vol. 8, pp. 313–326, June 1992.
- [16] S. Hutchinson, G. Hager, and P. Corke, "A tutorial on visual servo control," *IEEE Transactions on Robotics and Automation*, vol. 12, pp. 651–670, Oct. 1996.
- [17] G. Kantor and A. A. Rizzi, "Feedback control of underactuated systems via sequential composition: Visually guided control of a unicycle," in *2003, Proc. Int. Symp. on Robotics Research*, 2003.